  Bull. Chem. Soc. Jpn., 60, 3117—3124 (1987)

Effect of Molybdenum Codeposition on the Thermal Properties of Electroless Ni-B Alloy Plating Films

Tetsuya OSAKA,* Ichiro KOIWA, Keizo YAMADA, Masao NISHIKAWA, and Masahiko USUDA
Department of Applied Chemistry, School of Science and Engineering, Waseda University, Okubo, Shinjuku-ku, Tokyo 160
(Received March 12, 1987)

Electroless Ni-Mo-B alloy films from a bath using dimethylamine-borane(1/1) (DMAB) as a reducing agent were investigated. Only a small amount of Mo-complex addition to the bath decreased the boron content and increased the molybdenum content drastically. The maximum molybdenum content and maximum resistivity under as-plated conditions were obtained as 22.1 wt% and 322 μΩ cm respectively. Such a high resistivity is characteristic of Ni-Mo-B alloy films. Both crystallized and amorphous states of Ni-Mo-B alloy films, whose Mo contents were above 20 wt% with a small amount of boron, were prepared by controlling the Mo-complex concentration in the bath. The heat change properties of Ni-Mo-B alloy films were quite different from those of the electroless Ni alloy films reported previously. The resistivity of Ni-Mo-B alloy films after heat treatment at 500 or 600 °C became higher than that of those created under as-plated conditions. The structure transformation of Ni-Mo-B alloy films after heat treatment was quite different from that of ordinary electroless Ni alloy films. The Ni-Mo-B alloy film after heat treatment was confirmed by TEM observation to show a mosaic-like structure. Therefore, it was thought that such a high resistivity and such thermal properties of Ni-Mo-B alloy films are caused by such a mosaic-like structure.

In general, electroless nickel deposits contain P or B as impurities from reducing agents, and the properties of electroless alloy films depend strongly on the kind of reducing agent used.[1] It is also well known that a higher impurity content makes a film amorphous.[2-6] Since amorphous alloy films usually possess high resistivity and low temperature coefficient,[7] amorphous electroless Ni alloy films have a high possibility for use as thin film resistors. The amorphous films, however, are unstable because of these easy crystallization upon heat treatment. The high-melting-point element, molybdenum, has been reported to codeposit into electroless Ni films,[8-12] and the codeposition of Mo into the Ni films has the possibility of overcoming the demerit of its less stable thermal property. The present authors have previously attempted the Mo codeposition into Ni-P films on the basis of this point of view and have confirmed that the electroless plated Ni-Mo-P alloy film of a crystallized state has a thermal stability superior to that of amorphous and crystallized Ni-P film.[12]

In this paper, the present authors will report amorphous or crystallized electroless Ni-Mo-B alloy films of a high thermal stability, plated from a bath using dimethylamine-borane(1/1) (DMAB) as the reducing agent.

Experimental

Electroless Ni-Mo-B alloy films were plated from a caustic alkaline bath using dimethylamine-borane(1/1) (DMAB) as the reducing agent. The basic bath compositions and operating conditions are listed in Table 1. Molybdenum was easily codeposited by complexing sodium molybdate with sodium gluconate before constructing the bath by analogy to the method by Mallory.[10] The film thickness was adjusted to 2 μm by controlling the deposition time; however, in the case of transmission electron microscopy (TEM) measurement, the film thickness was adjusted to about 500 Å. Therefore, the initial deposition films were observed by means of TEM. Ninety six wt% alpha-alumina ceramics were used as a plating substrate except for the TEM measurement. For the TEM measurement, polyimide film (25KA, Toray Co. Ltd.) was used as a substrate, and the plated films were separated from the substrate by dipping the specimen in a hydrazine-ethylenediamine solution. The repeated two step process for catalyzation was used (sensitizer:$SnCl_2 \cdot 2H_2O$, 1 g dm^{-3}; 37% HCl, 1.0 ml dm^{-3}; activator:$PdCl_2$, 0.1 g dm^{-3}; 37% HCl, 0.1 ml dm^{-3}).[13] The contents of molybdenum and boron were determined by means of atomic absorption spectroscopy and the use of an inductively coupled argon plasma emission spectrophotometer (ICAP-575 markII, Nippon Jarrell-Ash). For the amorphous Ni-Mo-B alloy film, auger electron spectrometry (15-110A, PHI Co. Ltd.) was used to investigate such impurities as carbon and oxygen. The resistivity of deposits on the alumina substrate was measured by the four-probe method (MODEL K-705RD, Kyowa Riken Co. Ltd.). The structures of the deposits were determined by the use of an X-ray diffractometer (RAD-IIA,

Table 1. Electroless Plating Bath Compositions and Operating Conditions

Chemical	Concentration /mol dm^{-3}
$(CH_3)_2NH \cdot BH_3$	0.06
$C_3H_4(OH)(COONa)_3 \cdot 2H_2O$	0.10
$HOCH_2COOH$	0.20
$NiSO_4 \cdot 7H_2O$	0.05
Mo-complex	0—0.0125

Bath temperature, 90°C; pH adjusted with NaOH 9.0.

Rigaku Denki Co., Ltd.) and TEM measurement (100 kV, HU-12A, Hitachi Seisakusho Co., Ltd.). In the case of the heat treatment of deposits, the samples were heated under 2×10^{-3} Pa from room temperature to the setting temperature at a constant heating rate of 10 °C min^{-1}. The samples were heated for one hour at the setting temperature and were then left to cool spontaneously.

Results and Discussion

Film Composition and Resistivity of Electroless Plated Ni-Mo-B Alloy Films. The film composition and the resistivity as function of the Mo-complex concentration are listed in Table 2. The data of Ni-Mo-P alloy films were quoted from the previous paper[12] so as to compare them with those of Ni-Mo-B alloy films. In the case of Ni-Mo-B alloy films, the maximum Mo content and the highest resistivity value, 22.1 wt% and 322 μΩ cm respectively, were obtained at Mo-complex concentration of 0.0025 mol dm^{-3}. The highest resistivity value is about twice the value of a usual amorphous Ni-P alloy film. Moreover, the Mo content was almost independent of the Mo-complex concentration. This tendency was different from the case of Ni-Mo-P alloy films in the higher Mo-complex concentration region. On the other hand, the boron content was drastically decreased from 6.3 to 0.63 wt% by adding 0.0025 mol dm^{-3} Mo-complex. Moreover, the boron content gradually decreased with an increase in the Mo-complex concentration, and films with a very small 0.10 wt% B content were obtained at the region of a Mo-complex concentration of more than 0.0100 mol dm^{-3}. At the same Mo-complex concentration, the resistivity of Ni-Mo-B alloy film was always higher than that of Ni-Mo-P alloy film.

From the above results, there appears to be a difference between Ni-Mo-P alloy film and Ni-Mo-B alloy film under as-plated conditions. Especially, the Ni-Mo-B alloy film has the characteristics of a higher Mo content and a higher resistivity. In this paper, we mainly discuss the resistivity of Ni-Mo-B alloy film and its heat change properties, in particular, for the film at a Mo-complex concentration of 0.0025 mol dm^{-3}.

Heat Treatment Effect of Electroless Ni-Mo-B Alloy Film on Specific Resistance. Figure 1 demonstrates the effect of heat treatment on the specific resistance of Ni-Mo-B alloy films at Mo-complex concentrations of 0.0025 and 0.0125 mol dm^{-3}. The ρ value of Ni-B alloy film usually decreases with an increase in the heat treatment temperature as just as has been reported previously.[11] This tendency is generally found in Ni-P alloy films.[14]

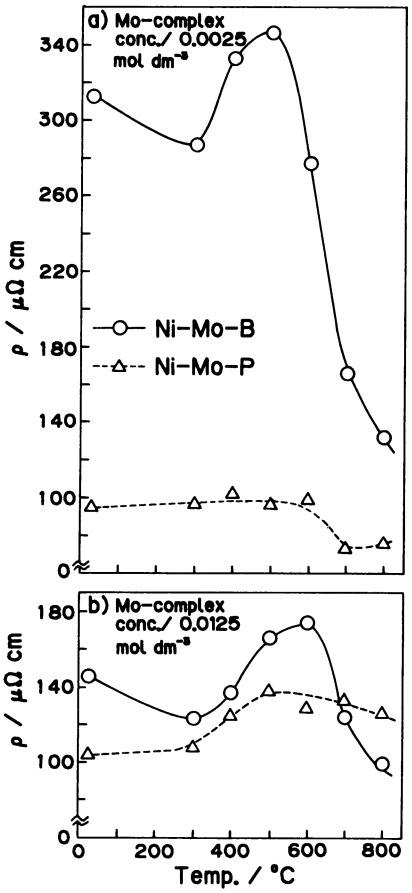

Fig. 1. Effect of heat treatment temperature on specific resistance, ρ. Solid line (circles): Ni-Mo-B. Dashed line (triangle): Ni-Mo-P.[12] a) 0.0025 mol dm^{-3} Mo-complex concentration, b) 0.0125 mol dm^{-3} Mo-complex concentration.

Table 2. Film Composition and Resistivity of Ni-Mo Alloy Films

Mo-complex conc. /mol dm^{-3}	Ni-Mo-B			Ni-Mo-P[12]		
	Mo/wt%	B/wt%	ρ/μΩ cm	Mo/wt%	P/wt%	ρ/μΩ cm
0	0	6.3	120	0	10.2	127
0.0025	22.1	0.63	322	10.0	2.0	95
0.0050	19.8	0.17	138	14.1	1.1	105
0.0075	21.5	0.12	130	14.8	0.98	101
0.0100	22.0	0.10	126	16.5	0.94	99
0.0125	21.1	0.10	146	16.5	0.95	104

The dashed lines are the data of Ni-Mo-P alloy films, quoted from a previous paper[12] for the sake of comparison. The ρ values of Ni-Mo-B alloy film at an Mo-complex concentration of 0.0025 mol dm^{-3} are always higher than those of Ni-Mo-P alloy films at any temperature. In Fig. 1a, the ρ value of Ni-Mo-B alloy film at a Mo-complex concentration of 0.0025 mol dm^{-3} after 300 °C heat treatment becomes a little lower than that of the as-plated conditions. In the heat treatment region from 300 until 500 °C, the ρ value increases with an increase in the heat treatment temperature; the maximum value of 347 $\mu\Omega$ cm was obtained after heat treatment at 500 °C. In the region higher than 500 °C, the ρ value drastically decreases with an increase in the heat treatment temperature. Even after heat treatment at 700 °C, however, the ρ value of Ni-Mo-B alloy film at the Mo-complex concentration of 0.0025 mol dm^{-3} is still higher than the maximum (150 $\mu\Omega$ cm) of electroless binary Ni alloy films. In the case of binary Ni alloy films, the maximum resistivity can be obtained only for the as-plated conditions. Therefore, the amorphous Ni-Mo-B alloy films showed a higher thermal stability of resistivity than did the previously reported binary Ni alloy films.

Moreover, the ρ value tendency of Ni-Mo-B at Mo-complex concentration of 0.0125 mol dm^{-3} is almost the same as that of Ni-Mo-B at the Mo-complex concentration of 0.0025 mol dm^{-3}, as is shown in Fig. 1b. From the above results, the ρ value behavior of amorphous and crystallized Ni-Mo-B alloy films after heat treatment is as follows: i.e., first there appears a little decrease at a low temperature heat treatment; then the ρ value increases in the region of medium-temperature heat treatment before decreasing abruptly at higher heat treatment temperatures.

The characteristics of three typical films are listed in Table 3. In general, a high resistivity film of the electroless plated one is obtained only for the films controlling high impurity. Though the boron contents of both Ni-Mo-B alloy films were very small, $\rho_{\text{as-plated}}$ and ρ_{maximum} values of the Ni-Mo-B alloy film

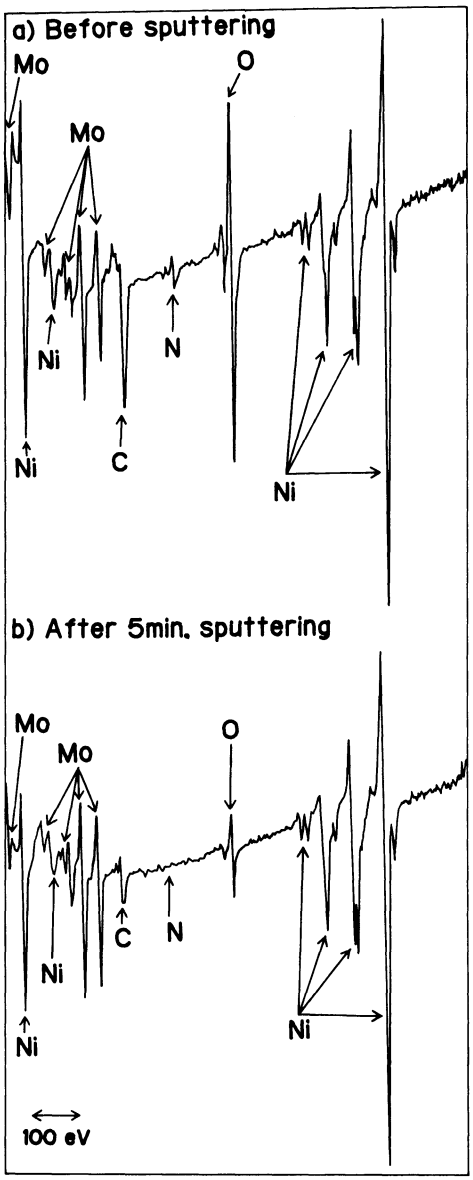

Fig. 2. Auger electron spectroscopy of amorphous Ni-Mo-B alloy films at 0.0025 mol dm^{-3} Mo-complex concentration. a) Before sputtering, b) after 5 min. sputtering.

Table 3. Characteristics of Typical Ni Alloy Films

Mo-complex conc. /mol dm^{-3}	$\rho_{\text{as-plated}}/\mu\Omega$ cm Structure	$\rho_{\text{maximum}}/\mu\Omega$ cm Their condition and structure
0	120 Amorphous	120 Under as-plated conditions Amorphous
0.0025	322 Amorphous	347 After 500°C treatment Almost amorphous
0.0125	146 Crystallized	176 After 600°C treatment Crystallized

are higher than those of the Ni-B alloy film. In particular, the maximum $\rho_{as\text{-}plated}$ value, 322 μΩ cm, is attained at the Mo-complex concentration of 0.0025 mol dm^{-3}. Moreover, the maximum ρ value, 347 μΩ cm, of electroless Ni-Mo-B alloy film was obtained by heat treatment at 500 °C. The heat treatment behavior of the ρ value of Ni-Mo-B alloy films is quite unique and can not be simply explained by the explanation given in the case of binary electroless plated film.[14]

Auger Electron Spectroscopy (AES) Analysis of the Ni-Mo-B Alloy Film. Figure 2 demonstrates the AES spectra of the Ni-Mo-B alloy film at the Mo-complex concentration of 0.0025 mol dm^{-3}. Before sputtering, the peaks corresponding to Ni, Mo, C, N, and O were detected. However, after 5 mins' sputtering, the peaks corresponding to C, N, and O remarkably decreased. The peak intensities of C and O after 5 mins' sputtering are almost the same as those of the other alloy, which means they come from the impurity. Thus, such a highly specific resistance of the Ni-Mo-B alloy film at the Mo-complex concentration of 0.0025 mol dm^{-3} is confirmed not to be the result of its containing an insulator composed of C and O atoms. The origin of such unique characteristics is assumed to come from a structure containing Mo atoms. Below, the structure of electroless Ni-Mo-B alloy films will be discussed.

The Effect of Heat Treatment on the Structure of Electroless Ni-Mo-B Film. Figure 3 demonstrates the X-ray diffraction patterns of Ni alloy films at Mo-complex concentrations of 0, 0.0025 and 0.0125 mol dm^{-3}. Under as-plated conditions, only the two peaks due to the substrate are detected for Ni-B and Ni-Mo-B alloy films at 0.0025 mol dm^{-3}, and they both show an amorphous structure. Amorphous binary alloy films, such as Ni-P and Ni-B alloy films, are usually obtained only in the case of films containing high P or B impurities. In fact, the Ni-B alloy film shows high boron content (6.3 wt%). On the other hand, Ni-Mo-B alloy film at the Mo-complex concentration of 0.0025 mol dm^{-3} shows the same X-ray pattern in spite of its quite low boron content (0.63 wt%). In contrast to the above two alloys, the Ni-Mo-B alloy film at the Mo-complex concentration of 0.0125 mol dm^{-3} shows a highly crystallized structure under as-plated conditions, since the peaks of the Ni matrix were detected, as is shown in Fig. 3c. Moreover, the peaks of the Ni(111) and Ni(200) plane shift to the lower angle side as compared with those of pure Ni; the interplanar spacing of the Ni-Mo-B film was widened by the codeposited Mo atoms. The molybdenum in the deposit may form a solid solution in the nickel matrix. The shift behavior of the Ni(111) plane peak is almost the same as that of Ni-Mo-P alloy film, but the amount of the shift is larger than that of Ni-Mo-P alloy film.[12] This large shift could be caused by the higher Mo content, as is shown in Table 2.

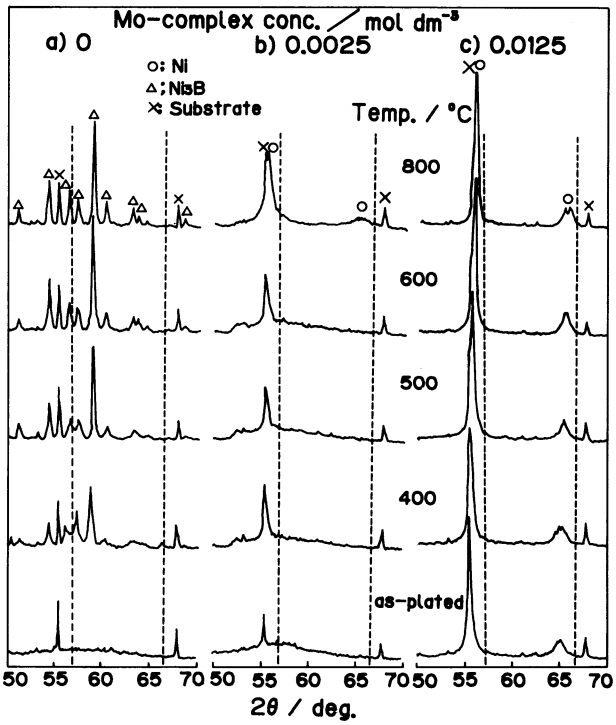

Fig. 3. X-Ray diffraction patterns of Ni-B and Ni-Mo-B alloy films at various annealing temperature using Fe target. The dashed lines represent the peak positions of pure Ni.
a) Ni-B alloy films, b) Ni-Mo-B alloy films plated from 0.0025 mol dm^{-3} Mo-complex concentration bath, c) Ni-Mo-B alloy films plated from 0.0125 mol dm^{-3} Mo-complex concentration bath.

Based upon the above results, we will now discuss the characteristics of electroless Ni-Mo-B alloy films under as-plated conditions in comparison with the results of the previous investigation. First, we will discuss the structures of electroless Ni-Mo-B alloy films. According to our previous investigation of electroless Ni-W-P alloy films, both amorphous and crystallized Ni-W-P alloy films with low P content could be prepared.[15,16] Therefore, the codeposited tungsten causes an amorphous state of the film. Since the boron content of amorphous Ni-Mo-B was extremely small, i.e., 0.63 wt%, the effect of the codeposited Mo atom in the Ni-B film is much greater than that of the codeposited W atom in the Ni-P film. In the case of highly crystallized Ni alloy films under as-plated conditions, the phenomenon of the d value shift, which may mean the formation of the solid solution between the codeposited atom and Ni matrix, can not be observed in the case of Ni-W-P alloy film,[15,16] but it can be observed in the case of Ni-Mo-P alloy film.[12] Therefore, the codeposited molybdenum can form a solid solution.

Next, we will discuss the resistivity of electroless

Ni-Mo-B alloy films. The amorphous Ni-P and Ni-W-P alloy films showed almost the same resistivity, i.e., about 150 μΩ cm, the highly crystallized Ni-P and Ni-W-P alloy films also show almost the same resistivity, i.e., about 50 μΩ cm. Therefore, the resistivities of the Ni-P and Ni-W-P alloy films depend strongly on the film structure. In the case of electroless Ni-Mo-B alloy films, the resistivities are much higher than those of Ni-P and Ni-W-P alloy films under the same structure conditions. Therefore, the resistivity of Ni-Mo-B alloy films can not be explained only by the structure. In general, amorphous alloys between transition metals, such as Zr-Ni[17] and Nb-Ni,[18] show a high resistivity above 200 μΩ cm. Therefore, in the case of amorphous Ni-Mo-B alloy film prepared by the electroless plating method, an effect similar to those of Zr-Ni and Nb-Ni is a possibility.

Based upon the above discussion, the amorphous and crystallized Ni-Mo-B alloy films are considered to be quite different from the amorphous and crystallized Ni-W-P alloy films. Therefore, the codeposited molybdenum is an important factor in determining the structure and resistivity. Moreover, the effect of codeposited molybdenum on film properties is different from that of codeposited tungsten.

In this investigation, three typical alloy films are obtained, i.e., the amorphous Ni-B, the amorphous Ni-Mo-B (plated from a 0.0025 mol dm^{-3} Mo-complex concentration bath), and the crystallized Ni-Mo-B (plated from a 0.0125 mol dm^{-3} Mo-complex concentration bath). These three typical alloy films will now be considered.

In the case of Ni-B alloy, only the peaks due to Ni_3B appear after heat treatment at 400 °C, as is shown in Fig. 3a, where the boron content of this amorphous Ni-B alloy film is almost the same as in the stoichiometric Ni_3B compound (6.3 wt%, i.e., 26.9 at%, see Table 2). The peak intensities gradually increase with an increase in the heat treatment temperature; indicates that the crystallinity of the Ni_3B compound progresses with heat treatment.

On the other hand, for the amorphous Ni-Mo-B alloy film, there is no structure change until 500 °C under heat treatment, as is shown in Fig. 3b, though an obvious structure change is observed after heat

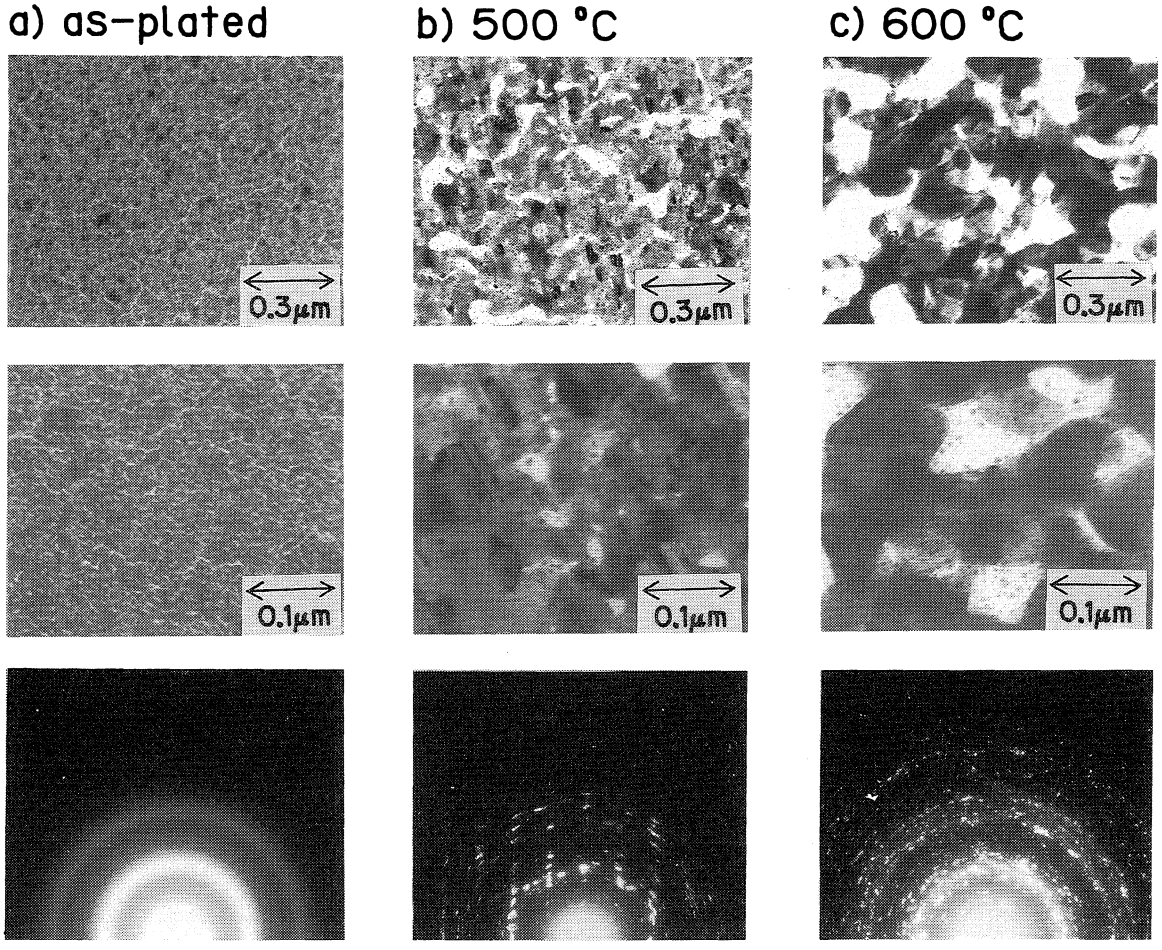

Fig. 4. Transmission electron micrographs (TEM) and transmission high energy electron diffraction (THEED) patterns of Ni-B alloy films. a) As-plated conditions, b) after 500 °C treatment, c) after 600 °C treatment.

treatment at 700 °C. In general, an amorphous alloy is very unstable against heat treatment; however, the thermal stability of this amorphous film has been improved by the codeposition of the Mo atom, much as in the case of Fe-Ni-Mo-B[19,20] and Cr-Mo[21] amorphous alloys. By considering the previous reported facts, such an excellent thermal stability of amorphous Ni-Mo-B alloy film may be assumed to be due to the codeposition of the Mo atom into Ni-B film.

For the crystallized Ni-Mo-B alloy film, the structure shows almost no change until heat treatment at 500 °C as is shown in Fig. 3c. The peak intensities gradually increase with an increase in the heat treatment temperature above 500 °C.

In the cases of both amorphous and crystallized Ni-Mo-B alloy films, the peaks of the Ni(111) and Ni(200) planes are shifted to a lower angle side than those of pure Ni. Thus, there is a stable solid solution between Mo and Ni.

Transmission Electron Microscopy (TEM) and Transmission High Energy Electron Diffraction (THEED) Measurement. Figures 4—6 demonstrate the TEM and THEED patterns for the films at the Mo-complex concentrations of 0, 0.0025, and 0.0125 mol dm^{-3}, respectively. Figure 4a demonstrates the TEM and THEED patterns of Ni-B alloy film under as-plated conditions. The TEM micrographs show an Ni-B alloy film consisting of very small grains, while the THEED pattern gives halo diffraction rings due to the Ni phase. After heat treatment at 500 °C, the film comes to consist of large grains, while the THEED pattern shows the formation of the Ni_3B compound, as is shown in Fig. 4b. After heat treatment at 600 °C, the contrast and the grain size become clearer and larger respectively. These results coincide well with results of the X-ray diffraction measurement. Therefore, a drastic structural transformation is produced by the heat treatment.

Figure 5 demonstrates the TEM and THEED patterns of amorphous Ni-Mo-B alloy film with the same arrangement as is shown in Fig. 4. The results of the TEM and THEED of amorphous Ni-Mo-B alloy film under as-plated conditions are almost the same as those of Ni-B alloy film, as is shown in Fig. 4a. Broad

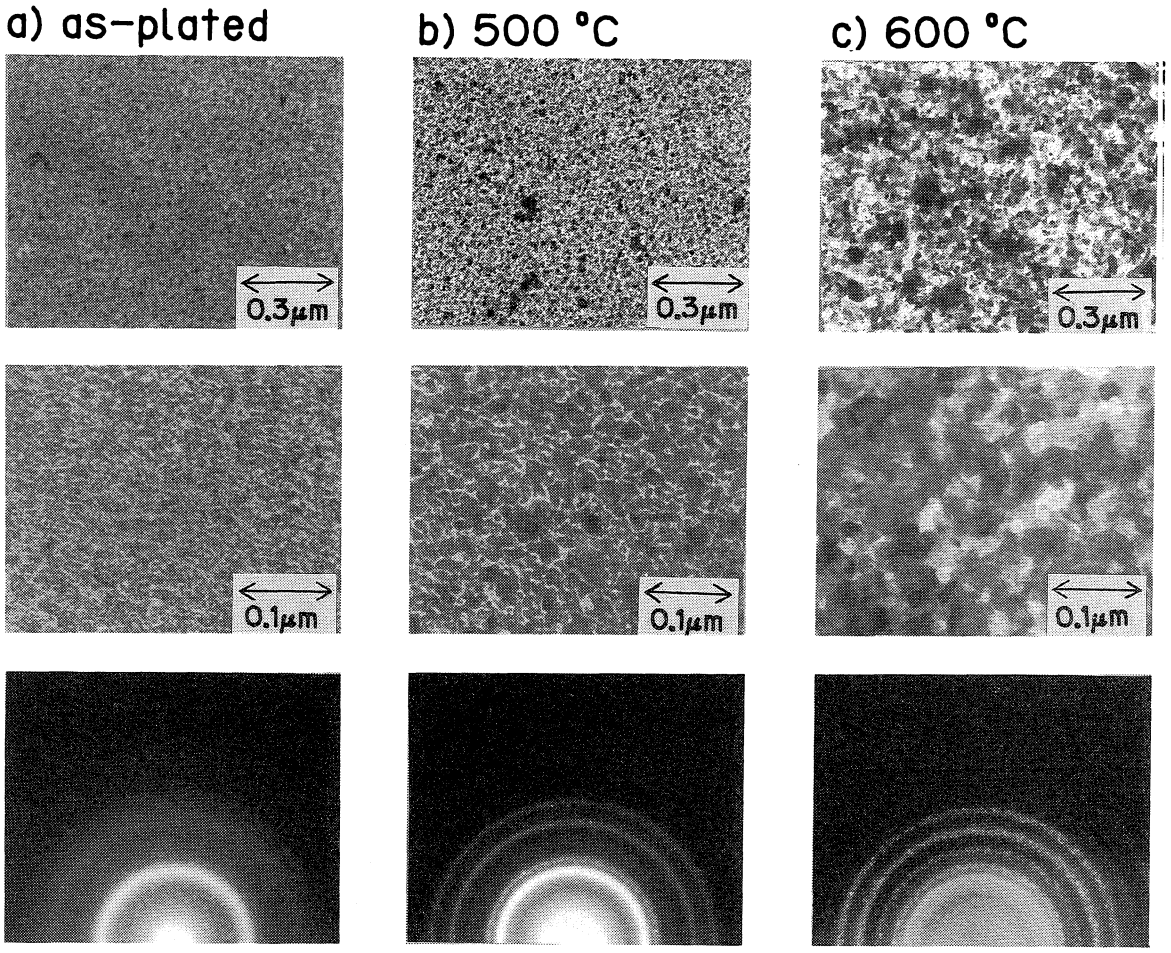

Fig. 5. Transmission electron micrographs (TEM) and transmission high energy electron diffraction (THEED) patterns of Ni-Mo-B alloy films at 0.0025 mol dm^{-3} Mo-complex concentration. a) As-plated conditions, b) after 500 °C treatment, c) after 600 °C treatment.

diffraction rings due to the Ni-Mo alloy are observed under as-plated conditions, and the grain sizes become a little larger after heat treatment at 500 °C treatment. The crystallinity after treatment at 500 °C is not so high, judging from the wider width of the diffraction rings. After heat treatment at 600 °C, the contrast and the grain sizes increase, and there appears a mosaic-like structure; however, the width of the diffraction rings is still wider.

Figure 6 demonstrates the TEM and THEED patterns of crystallized Ni-Mo-B alloy film in the same manner as in Figs. 4 and 5. The same tendency as that in Fig. 5 is observed. As is also seen in the X-ray diffraction measurement results in Fig. 3c, the crystallization proceeds gradually with an increase in the heat treatment temperature. The diffraction rings became sharper after heat treatment at 500 °C. The grain sizes after heat treatment at 600 °C are almost the same as those after heat treatment at 500 °C, only the contrast between 500 and 600 °C becomes clearer.

In general, the crystallized film after heat treatment shows large grown-grains and sharp diffraction rings. In contrast with the usual case, the heat change behavior of electroless Ni-Mo-B alloy films is quite different. Such a mosaic-morphology and broad diffraction rings after heat treatment are characteristic of the Ni-Mo-B alloy film. The usual crystallization process is accompanied by an increase in grain size, and finally the grown-grains combine with each other, thus making possible a free path of electrons.[14] Therefore, the resistivity is usually decreased by the normal crystallization process after heat treatment. In contrast with such a usual crystallized film, the crystallized Ni-Mo-B alloy is crystallized by heat treatment, without any accompanying increase in grain size. The grains are still clearly separated, even after treatment at 600 °C, and such a formation of a grain matrix does not permit a free path for electrons. Thus, the characteristics of such a mosaic-like structure are assumed to be the origin of the high resistivity and high thermal stability. Moreover, in the case of amorphous Ni-Mo-B alloy films, these characteristics are enhanced.

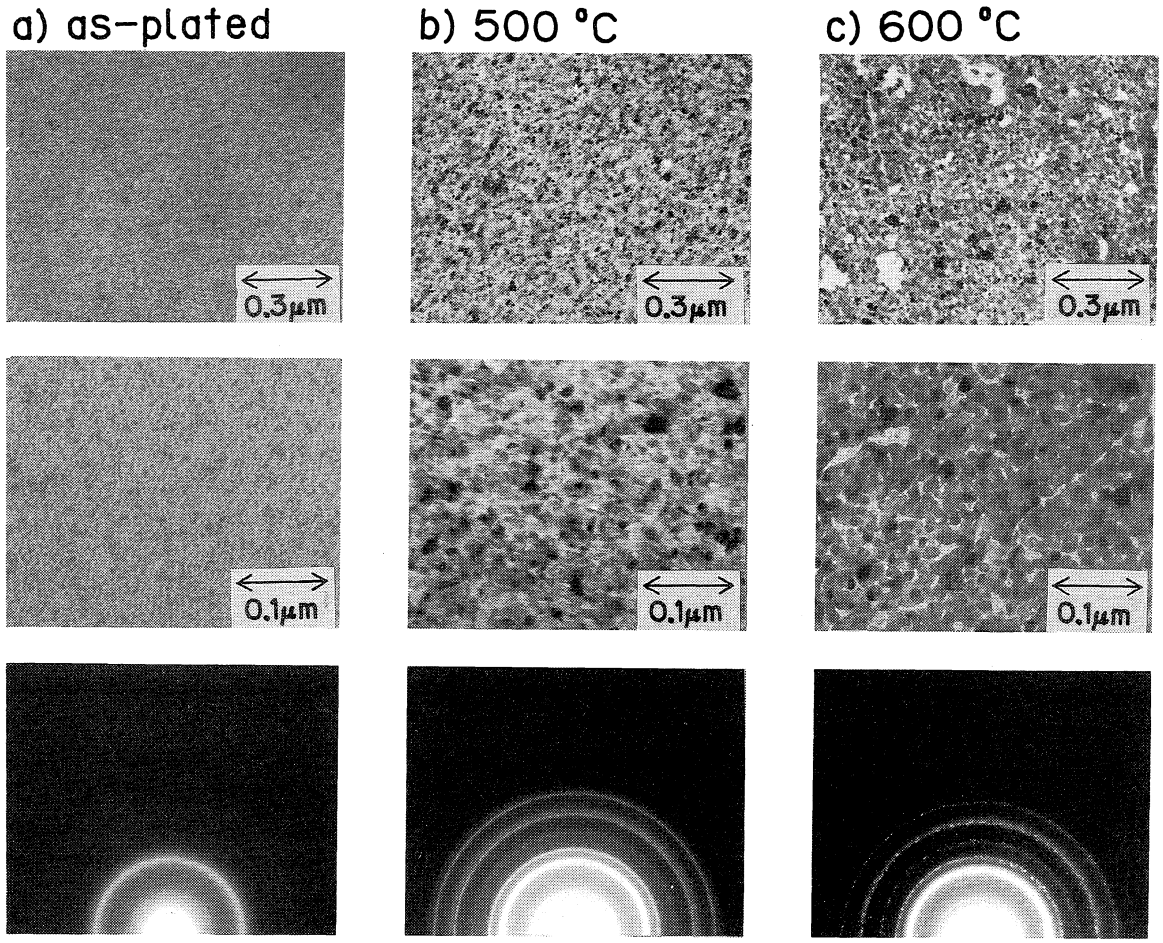

Fig. 6. Transmission electron micrographs (TEM) and transmission high energy electron diffraction (THEED) patterns of Ni-Mo-B alloy films at 0.0125 mol dm^{-3} Mo-complex concentration. a) As-plated conditions, b) after 500 °C treatment, c) after 600 °C treatment.

Conclusion

Electroless Ni-Mo-B alloy films, which had been prepared from a bath using dimethylamine-borane (1/1) (DMAB) as the reducing agent, were studied from the viewpoint of forming thermally stable film. The following results were obtained:

1) Amorphous and crystallized Ni-Mo-B alloy films with Mo contents of more than 20 wt% were obtained from an electroless plating bath.

2) The maximum molybdenum content and the very high resistivity value of Ni-Mo-P film were 22.1 wt% and 322 μΩ cm respectively under as-plated conditions. The origins of such a high resistivity value of Ni-Mo-B alloy film were assumed to be the formation of a solid solution and the unique microstructure.

3) The maximum resistivity of electroless Ni-Mo-B alloy films was obtained after heat treatment. After heat treatment at 500 °C, the maximum resistivity of 347 μΩcm was obtained for the film plated from a 0.0025 mol dm^{-3} Mo-complex concentration bath.

4) The microstructure of Ni-Mo-B alloy film, with a high resistivity, after heat treatments at 500 and 600 °C was due to an unique mosaic-like structure.

The authors are indebted to the financial support of the Asahi Glass Foundation for Industrial Technology.

References

1) E.g., F. Pearlstein, "Electroless Plating," in (F. A. Lowenheim, ed.) Modern Electroplating, 3rd ed., John Wiley & Sons, New York (1974), Chap. 31.

2) A. W. Goldstein, W. Rostoker, F. Schossberger, and G. Gutzeit, *J. Electrochem. Soc.*, **104**, 104 (1957).

3) J. P. Marton and M. Schlesinger, *J. Electrochem. Soc.*, **115**, 16 (1968).

4) K. M. Gorbunova, M. V. Ivanov, and V. P. Moiseev, *J. Electrochem. Soc.*, **120**, 613 (1973).

5) T. Watanabe and Y. Tanabe, *J. Jpn. Inst. Metals*, **39**, 831 (1975).

6) H. Suda, T. Watanabe, and Y. Tanabe, *J. Jpn. Inst. Metals.*, **45**, 5 (1981).

7) E.g., P. T. Cote, *Solid State Communications*, **18**, 1311 (1976).

8) G. O. Mallory, *Plating and Surface Finishing*, **63** (6), 34 (1976).

9) M. Schwartz and G. O. Mallory, *J. Electrochem. Soc.*, **123**, 606 (1976).

10) G. O. Mallory and T. R. Horhn, *Plating and Surface Finishing*, **66** (4), 40 (1979).

11) I. Koiwa, M. Nishikawa, K. Yamada, and T. Osaka, *Denki Kagaku*, **53**, 510 (1985).

12) I. Koiwa, M. Nishikawa, K. Yamada, and T. Osaka, *Bull. Chem. Soc. Jpn.*, **59**, 133 (1986).

13) L. G. Svendsen, T. Osaka, and H. Sawai, *J. Electrochem. Soc.*, **130**, 2252 (1983).

14) E.g., S. T. Pai, J. P. Marton, and J. D. Brown, *J. Appl. Phys.*, **43** (2), 282 (1972).

15) I. Koiwa, T. Osaka, and H. Sawai, *Kinzoku Hyomen Gijutsu*, **34**, 600 (1983).

16) H. Sawai, T. Kanamori, S. Shibata, K. Nihei, T. Osaka, I. Koiwa, and M. Nishikawa, Proc. of 11th Inter. Cong. of Metal Finishing, Israel (Oct. 1984), p. 323.

17) K. H. J. Buschow and N. M. Beekmans, *Phys. Rev.*, **B19**, 3843 (1979).

18) S. R. Nagel, J. Vassilion, P. M. Horn, and B. C. Giessen, *Phys. Rev.*, **B17**, 462 (1978).

19) P. Allia, D. Andreone, R. S. Turtelli, F. Vinai, and G. Riontino, *J. Appl. Phys.*, **53**(12), 8798 (1982).

20) C. Antonione, L. Battezzati, A. Lucci, G. Riontino, M. C. Tabasso, and G. Venturello, *J. de Phys.*, **C8**, 131 (1980).

21) H. Furuya, N. Hasegawa, Y. Misaki, and Y. Tanabe, *Kinzoku Hyomen Gijutsu*, **32**, 637 (1981).